Diffraction Limited Polarimetry from the Infrared Imaging Magnetograph at Big Bear Solar Observatory

Wenda Cao[1,2], Ju Jing[1,2], Jun Ma[1], Yan Xu[1], Haimin Wang[1,2], and Philip R. Goode[1,2]

1. Center for Solar-Terrestrial Research, New Jersey Institute of Technology 323 Martin Luther King Blvd, Newark, NJ 07102

2. Big Bear Solar Observatory, 40386 North Shore Lane, Big Bear City, CA 92314

wcao@bbso.njit.edu

ABSTRACT

The InfraRed Imaging Magnetograph (IRIM) system developed by Big Bear Solar Observatory (BBSO) has been put into preliminary operation. It is one of the first imaging spectro-polarimeters working at 1.56 μm, and is used for the observations of the Sun at its opacity minimum, exposing the deepest photospheric layers. The tandem system of a 42 Å interference filter, an unique 2.5 Å birefringent Lyot filter and a Fabry-Pérot etalon is capable of providing a bandpass as low as 0.1 Å in a telecentric configuration. A fixed quarter wave plate and a nematic liquid crystal variable retarder are employed for analyzing the circular polarization of the Zeeman components. The longitudinal magnetic field is measured for highly Zeeman-sensitive Fe I line at 15648.5 Å (Landé factor $g = 3$). The polarimetric data, with a field of view (FOV) $\sim 145'' \times 145''$, were recorded by a 1024×1024 pixel, 14-bit HgCdTe CMOS focal plane array camera. Benefiting from the Correlation Tracking system (CT) and newly developed Adaptive Optics (AO) system, the first imaging polarimetric observations at 1.56 μm were made at the diffraction limit on 1 July 2005 using BBSO's 65 cm telescope. After comparing the magnetograms from IRIM with those taken by the Michelson Doppler Imager (MDI) on board *SOHO*, it was found that all the magnetic features matched very well in both sets of magnetograms. Also, Stokes V profiles obtained from the Fabry-Pérot etalon scanning data provide access to both the true magnetic field strength and filling factor of the small-scale magnetic flux elements. In this paper, we present the design, fabrication, and calibration of IRIM, as well as the results of the first scientific observations.

Subject headings: Sun: magnetic fields – Sun: infrared – Instrumentation: spectro-polarimeter

1. Introduction

It has been widely accepted that the small-scale magnetic field concentrations rooted in the deepest layers of solar photosphere play a crucial role in the physical processes driving solar activity and variability. Typical magnetic flux elements are believed to exist in kilogauss-strength magnetic concentrations with a characteristic size $\leq$ 100 km at the base of photosphere (Rimmele 2004). The dynamic studies of these flux concentrations require two-dimensional polarimetry with high magnetic sensitivity, as well as high spatial and temporal resolution. As a result, two categories of spectro-polarimeters have been developed and widely utilized in the observations of the visible wavelength for decades. The classical spectrograph based systems are capable of providing high spectral resolution. Since two-dimensional polarimetry is realized by scanning the image across the entrance slit of the spectrograph, these instruments are severely limited in spatial and temporal resolution. Filter based systems typically offer better spatial resolution, while moderate spectral resolution is the drawback of these instruments. However, due to the recent advances in Fabry-Pérot interferometer technologies, the spectral resolution $\lambda/\delta\lambda$ of such tunable systems can also reach up to $10^{5\sim6}$. Many Fabry-Pérot based filter spectro-polarimeters (Mickey et al. 1996; Bonaccini et al. 1990; Bendlin et al. 1995; Koschinsky et al. 2001; von der Lühe 2000) operating in the visible wavelength range have demonstrated their importance and bright future in the last decade. Even so, it is relatively unusual to acquire diffraction limited observations of small-scale features with sub-arc spatial resolution and high polarization accuracy (Keller and von der Lühe 1992; Rimmele 2004).

The Near InfraRed (NIR) provides a promising tool to probe the small-scale solar magnetic features for the following reasons: (1) The Fried parameter, isoplanatic angle, and Greenwood time delay are all proportional to $\lambda^{6/5}$. The angular seeing at 1.56 μm is at least 4 times better than in the visible under the same observational condition; (2) The Zeeman splitting is a function of $g\lambda^2 B$. Even a moderate magnetic field can cause full line splitting in NIR, allowing magnetic field measurement of high sensitivity. Meanwhile, the cross-talk between the Stokes V and Stokes Q or U component induced by instrument is suppressed tremendously in the NIR; (3) The opacity due to H^- absorption reaches its minimum at 1.6 μm. Therefore, the deepest layers of photosphere can be probed by virtue of the 1.6 μm opacity minimum; (4) The scattering light from both the atmosphere and telescope are tremendously reduced in the NIR. The Near-Infrared Magnetograph (NIM-I) (Rabin 1992a,b) is the first spectrograph based polarimeter working at 1.56 μm, which combines the advantages of infrared Zeeman-sensitivity with the capability of spatial mapping. Since the NIM-I, many NIR spectroscopic and polarimetric observations have been carried out with a variety of spectrographs by a number of authors (Penn et al. 2002, 2003; Bellot Rubio et al. 2000; Lin et al. 1999; McPherson et al. 1992; Solanki et al. 1993; Kopp et al. 1992). NIM-II

and the dual NIR Fabry-Pérot etalon system of NSO are two early attempts at filter based systems. Despite all of these efforts, none of the previous NIR imaging systems produced magnetograms, let alone the observations under diffraction limited conditions.

IRIM is one of the first filter based spectro-polarimeters operating in the NIR. Along with the Visible Imaging Magnetograph (VIM) at BBSO, it will be the most important post-focus instrument of the 65 cm telescope and in the near future, the 1.6 m New Solar Telescope under development at BBSO. The design concept has been described by Denker et al. (2003). An interference filter, a birefringent Lyot filter, and a Fabry-Pérot etalon in tandem are combined to obtain ~ 0.1 Å bandpass over a FOV of $145'' \times 145''$ in a telecentric configuration. The design goal is to acquire the images of high spatial resolution (close to the diffraction limit $\sim 0.62''$), high temporal resolution ($\sim$ 1-2 min), and moderate spectral resolution ($\sim 10^5$). It will provide four operating modes: polarimeter mode (full spectral profile with polarization optics), spectrometer mode (full spectral profile without polarization optics), Doppler mode (a few selected spectral points), and photometric mode (single spectral point). After calibrating each optical component, the first diffraction limited imaging polarimetry using the Fe I 15648.5 Å line was made on 1 July 2005 with the high order AO system of BBSO. In this paper, we present the detailed design of the instrumentation and discuss the preliminary results of the observations.

2. Instrumentation

The post-focus instruments including AO, IRIM, and VIM at BBSO are arranged on a stable optical table in a temperature controlled Coudé room, with the relevant optical layout shown in Figure 1. A set of relay optics deliver sunlight from the 65 cm telescope into the Coudé room. The telescope pupil is imaged on a deformable mirror (DM). A dichroic beam splitter (BS1) splits the solar beam reflected by DM into two individual channels for IRIM and VIM. The beam size is reduced by a positive lens L8 and a negative lens L9 from 77 mm to a suitable size to pass through the interference filter, the polarization analyzer, and the birefringent Lyot filter. Further, these two lenses slow the beam to a f-number of 120 to minimize the bandpass broadening of Fabry-Pérot etalon. Another positive lens L10 makes an exact telecentric configuration for Fabry-Pérot etalon. An image with a FOV of $145'' \times 145''$ is re-imaged onto FPA by lens L11.

The NIR detector is a HgCdTe CMOS focal plane array (FPA) camera with image sensor chip TCM8600 manufactured by Rockwell Scientific Company (Cao et al. 2005a). The FPA based on a liquid nitrogen cooling system has 1024×1024 pixels, 100% filling factor, and a quantum efficiency $\geq 50\%$ in NIR. Eight readout channels ensures a transfer speed of up

to 30 frames per second. The output signal is digitalized into 14-bit with a dynamic range better than 70 dB. The pixel size is 18 μm $\times$ 18 μm.

A 70 mm aperture, ET70FS-1041 Series II Fabry-Pérot etalon manufactured by Queesgate Instruments Ltd. is operated by a CS-100 controller (SN 8105) to acquire narrow bandpass transmission and wavelength tunability. To eliminate the impact of fluctuations of ambient pressure, humidity, and temperature, as well as contamination of dust particles on it, the etalon is mounted in a sealed cell with two anti-reflection coated windows. A glass reference capacitor is employed to improve stability in controlling the cavity spacing and the etalon parallelism. According to the manufacturer's specifications, the cavity scanning range is larger than 4.1 μm, and the reflectivity is over 94% in the wavelength range from 1.0 μm to 1.6 μm. Some important performance parameters at 1.565 μm have been evaluated and measured by using a He-Ne laser and a horizontal spectrograph respectively (Cao et al. 2003). The relevant characteristic parameters of IRIM Fabry-Pérot etalon are summarized in Table 1.

As shown in Table 1, the free spectral range (FSR) of the Fabry-Pérot etalon, i.e., the distance between consecutive transmission peaks is about 5.5 Å at 1.565 μm. The birefringent Lyot filter (Wang et al. 2000) was designed to be the order sorting filter for the Fabry-Pérot etalon. Four stacks of calcite module sandwiched between linear polarizers are combined to acquire $\sim$ 2.5 Å bandpass with a diameter of 36 mm. The wide field configuration used in design tolerates up to 2° incidence angle. The nematic liquid crystal variable retarders (LCVR) are attached to each stack to tune the bandpass in range of $\pm$ 100 Å. To avoid a drift of the central bandpass due to variation in the ambient temperature, the whole system is enclosed in a thermal controller. The temperature is maintained at 32°C with a stability $\pm$ 0.1°C. The calibration and characteristic evaluations have been performed by using the horizonal spectrograph at the Evan's Facility of NSO, Sacramento Peak by Cao et al. (2005b). The working voltages of four LCVRs for each stack were determined at 15648.5 Å. The measured FWHM and FSR are 2.46 Å and 39.75 Å respectively. The measured transmission is about 15.9% for the unpolarized beam.

A NIR interference prefilter is utilized to isolate the transmissions from the sidelobe peaks of the birefringent Lyot filter. The transmission profile was measured by using the main spectrograph of the McMath-Pierce Telescope of NSO, Kittpeak. The result showed that this 3-cavity interference filter provides a bandpass with FWHM of 42.2 Å, which is able to reduce the sidelobe contamination to a very low level ($< 1\%$).

A fixed $\lambda/4$ wave plate, a LCVR, and NIR linear polarizer constitute the polarization analyzer for measuring the longitudinal magnetic field by using the high Zeeman-sensitivity of the Fe I 15648.5 Å line. Because the transmission axis of the five NIR polarizers inside

the birefringent Lyot filter are parallel to each other, the filter itself is a linear polarizer, as well. The fast axis of the fixed $\lambda/4$ wave plate and the LCVR are oriented at 45° to the polarization axis of the birefringent Lyot filter. The left and right circular Zeeman components are converted to orthogonal states of linear polarization by the initial fixed $\lambda/4$ wave plate. The modulator uses a LCVR from Meadowlark Optics, which is electrically switched between 0λ and $\lambda/2$. One of the components is blocked by the succeeding linear polarizer allowing the selected image corresponding to $I+V$ or $I-V$ in the emerging beam. The instrumental polarization of the telescope and other reflecting surfaces has not been modelled, therefore, observations of Stokes Q and U are not possible at this time.

3. Observations

The CT system and high-order AO system developed jointly by NSO and BBSO have been put into routine observation (Didkovsky et al. 2003; Rimmele 2000; Rimmele et al. 2003). The CT system uses a 45 mm diameter two-axis tip/tilt mirror with a resonance frequency around 3.3 kHz and tilt range of 25″. The AO system consists of a 77 mm diameter DM with 97 actuators and a Shack-Hartman wavefront sensor with 76 subapertures. Because of atmospheric stability in the NIR, diffraction limited polarimetry is often achieved at BBSO over IRIM's FOV in the NIR, while the effect of seeing induced cross-talk is suppressed significantly.

On 1 July 2005, imaging polarimetric observations of NOAA Active Region (AR) 10781 were first made using IRIM with combination of the CT and AO systems. The image scale was 0.142″ per pixel. The data were over-sampled by a factor of 2.18 of the diffraction limit at 1.565 μm for the BBSO's 65 cm solar telescope. The alternating frames of left-handed and right-handed circularly polarized images were acquired by switching the modulator from 0λ to $\lambda/2$. These images were stored in separate memory buffers of the image acquisition system. A number of images were added in the respective buffers to achieve a sufficiently high signal to noise ratio. Because of the high Zeeman-sensitivity of the Fe I line at 15648.5 Å, as little as 40-frame integration is capable of providing an acceptable signal to noise ratio. Each image is formed by differencing the above-mentioned component pairs and dividing by the sum of them. The exposure time is 200 millisecond for individual frame. So, each 40-frame integrated Stokes V image at each specific wavelength takes about 20 seconds. Figure 2 shows a sample magnetogram and the corresponding Stokes I image of NOAA AR 10781 taken at 16:00 UT.

Magnetograms have different sensitivities at different wavelengths in the same spectral line. It is necessary to search for the most sensitive wavelength region in blue wing of the

spectral line. Similar to the old BBSO vidiomagnetograph, the bandpass of IRIM can be fixed at a certain wavelength for tracking rapid changes in magnetic flux density. On the other hand, Stokes V profiles are obtained by scanning magnetograms across the line. These profiles provide the information needed to calculate the true magnetic field strength and the filling factor of the small-scale magnetic flux elements. Hence, IRIM provides two operating modes for acquiring magnetograms: the single bandpass mode to monitor rapid magnetic changes and the scanning mode to obtain the true field strengths. The spectro-polarimetric observations of the aforementioned AR were carried out by tuning the Fabry-Pérot etalon from -1.16 Å (*blue wing*) to +1.16 Å (*red wing*) from the line center in steps of 58 mÅ. Figure 3 shows a spectral sequence of the magnetograms of NOAA AR 10781 on 1 July 2005.

4. Results

The most sensitive response for the network magnetic fields is found when the pass-band is blue-shifted away from the Fe I line center by 0.46 Å. In order to demonstrate the validity of the measurement, we compared our results with the corresponding SOHO/MDI magnetograms. Figure 4 shows the MDI magnetogram of NOAA AR 10781 obtained around the same time. It is very clear that all the magnetic features matched very well in both of the magnetograms. Moreover, the magnetogram from IRIM reveals the small scale features with sub-arcsecond resolution. After accurate alignment and degrading IRIM's image scale to match that of MDI, we plot the scatter diagram and depict it in Figure 4. The plot shows the consistency of two magnetograms from IRIM and MDI. The deviations may be attributed to the use of different spectral lines and difference in spectral and spatial resolution in the two instruments.

After accurate alignment for each magnetogram at different wavelength, the Stokes V profile for each resolution element can be constructed. This profile provides an input to measure the true field strength and the filling factor. The inversion of stokes V profiles for each magnetic element is based on Unno-Rachkovsky theory. The analytic solution of the transfer equation for polarized radiation for Stokes parameters in a Milne-Eddington atmosphere was first given by Unno (Unno, W. 1956) and later by Rachkovsky, who added magneto-optical effects into consideration. We used an Unno fitting code based upon an iterative non-linear least squares algorithm, to fit to the polarization profiles and retrieve the input magnetic field. The inversion for the magnetic field was performed by minimizing the difference between observed Stokes profiles and the profiles described by Unno-Rachkovsky solution. Due to the limitation of available liquid crystals thus far, only stokes V and I parameters were measured and included in the fitting. Stokes Q and U variables are ignored

in the calculation of χ^2 and the minimization procedure by setting the dummy variables to be zero. The fitted results are required to satisfy the following criteria before being accepted for further analysis: (1) The algorithm must return an covariance matrix of the fitted quantities, i.e., the χ^2 value changes by a convergence tolerance of 10^{-4}; (2) Considering background noise, 2×10^{16} Mx, is considered to be the detectable minimum magnetic flux density. Figure 5 depicts the Stokes V profile over $\pm$ 1.16 Å of a magnetic element. The arrows point to the corresponding locations in I and V/I images respectively. The fitted Stokes V profile is overplotted also. The fitted intrinsic magnetic field strength is 482 gauss with a filling factor of 49.3%. The inversion procedure was applied to the observed region. Figure 6 shows the true-field, true-flux, and filling factor maps of the AR. Those pixels where the fitting results did not satisfy the convergence and signal-to-noise criteria are set to zero.

This diffraction limited polarimetry has revealed many dynamic phenomena of small-scale features. Figure 7 shows such an example for detailed view. Although the dust on the surfaces of the Fabry-Pérot etalon are difficult to clean by the dark and flat field corrections because of the telecentric configuration, some small-scale magnetic features, such as small pores (marked by p), magnetic knots (marked by k), etc. are clearly identified in the Stokes I and V/I images in Figure 7. We also found two regions with strong magnetic fields (marked by u), yet no corresponding to specific features were discovered in the I image. This discrepancy was observed by Keller (1995) and Wang et al. (1998), as well. In addition, there is a kind of small-scale magnetic structure (marked by e) of special interest. These features exist in a form of elongated magnetic structure along the dark intergranular lanes with $\sim 0.5'' \times 2''$ characteristic size and 150$\sim$300 gauss magnetic field. We will engage the dynamics of these features in more detail in subsequent observations.

5. Summary

An imaging spectro-polarimeter based on the Fabry-Pérot etalon has been designed, calibrated, and put into routine observation of Stokes V at BBSO. This is the first working filter-based magnetograph system in NIR. The diffraction limited polarimetry was achieved with assistance of CT and AO systems using the highly Zeeman-sensitive Fe I line at 15648.5 Å. The comparison of IRIM magnetograms with MDI data illustrates a good consistency between them. The Stokes V profile from rapid scanning across the spectral line provides access to measuring the true field strength and filling factor using the Stokes inversion method. The preliminary data analysis demonstrates the capability of IRIM in acquiring high spatial and temporal resolution, and high Zeeman sensitivity data, which can be used to probe the small-scale dynamic phenomena of the deepest observable levels of the photosphere.

We acknowledge the contributions of Denker, C., Wang, J., Hartkorn, K., Spirock, T., Nenow, J. of BBSO/NJIT. Also, we would like to thank Rimmele, T. at Sacpeak/NSO and Livingston, W. at Kittpeak/NSO for their help in the instrument calibration. The National Solar Observatory is a Division of the National Optical Astronomy Observatories, which is operated by the Association of Universities for Research in Astronomy, Inc., under cooperative agreement with the National Science Foundation. Our work is supported by NSF under grant ATM-0342560 and NASA under grant NAS5-12782.

REFERENCES

Bellot Rubio, L. R., Collados, M., Cobo, R., Rodriguez Hidalgo, I. 2000, ApJ, 534, 989

Bendlin, C., Volkmer, R., 1995, A&AS, 112, 371

Bonaccini, D., Stauffer, F. 1990, A&A, 217, 368

Cao, W., Denker, C., Wang, H., Ma, J., Qu, M., Wang, J., Goode, P. R. 2003, Proc. SPIE, 5171, 307

Cao, W., Xu, Y., Denker, C., Wang, H. 2005, Proc. SPIE, 5881, 245

Cao, W., Hartkorn, K., Ma, J., Xu, Y., Wang, J., Spirock, T., Wang, H. 2005, to be submitted to Sol. Phys.

Denker, C., Ma, J., Wang, J., Didkovsky, L., Varsik, J., Wang, H., Goode, P. R. 2003, Proc. SPIE, 4853, 223

Didkovsky, L. V., Dolgushyn, A. I., Marquette, W. H., et al. 2003, Proc. SPIE, 4853, 630

Keller, C. U. 1995, Rev. Mod. Astron., 8, 27

Keller, C. U. and von der Lühe, O. 1992, A&A, 261, 321

Kopp, G and Rabin, D. 1992, Sol. Phys., 141, 253

Koschinsky, M., Kneer, F., Hirzberger, J. 2001, A&A, 365, 588

Lin, H., Rimmele, T. R. 1999, ApJ, 514, 448

McPherson, M. R., Lin, H., Kohn, J. R. 1992, Sol. Phys., 139, 255

Mickey, D. L., Canfield, R. C., LaBonte, B. J., Leka, K. D., Waterson, M. F.,Weber, H. M. 1986, Sol. Phys., 168, 229

Penn, M. J., Ceja, J. A., Bell, E., Frye, G., Linck, R. 2002, Sol. Phys., 205, 53

Penn, M. J., Cao, W. D., Walton, S. R., Chapman, G. A., Livingston, W. 2003, Sol. Phys., 215, 87

Rabin, D. 1992, ApJ, 390, L103

Rabin, D. 1992, ApJ, 391, 832

Rimmele, T. R. 2000, Proc. SPIE, 4007, 218

Rimmele, T. R., Richards, K., Hegwer, S. L., Ren, D., Fletcher, S., Gregory, S., Didkovsky, L. V., Denker, C., Marquette, W., Marino, J., & Goode, P. R. 2003, Proc. SPIE, 4839, 635

Rimmele, T. R 2004, ApJ, 604, 906

Solanki, S. K., Walther, U., Livingston, W. 1993, A&A, 277, 639

Unno, W. 1956, PASJ, 8, 108

von der Lühe, O., Kentischer, T. J. 2000, A&AS, 146, 499

Wang, H., Denker, C., Spirock, T. J., Goode, P. R., Yang, S., Marquette, W., Varsik, J., Fear, R. J., Nenow, J., Dingley, D. D. 1998, Sol. Phys., 183, 1

Wang, J., Wang, H., Spirock, T. J., Lee, C. Y., Ravindra, N. M., Ma, J., Goode, P. R., Denker, C. 2000, Opt. Eng., 40, 1016

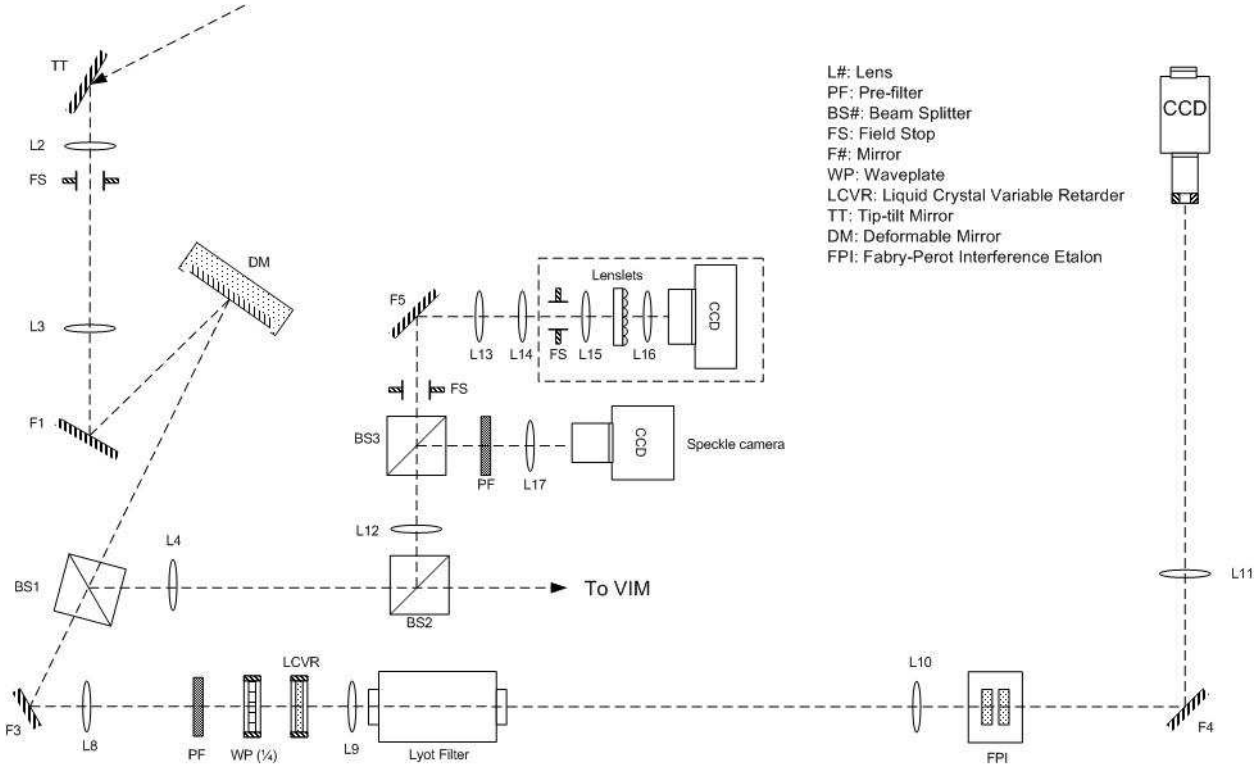

Fig. 1.— Optical layout of BBSO's IRIM and AO system.

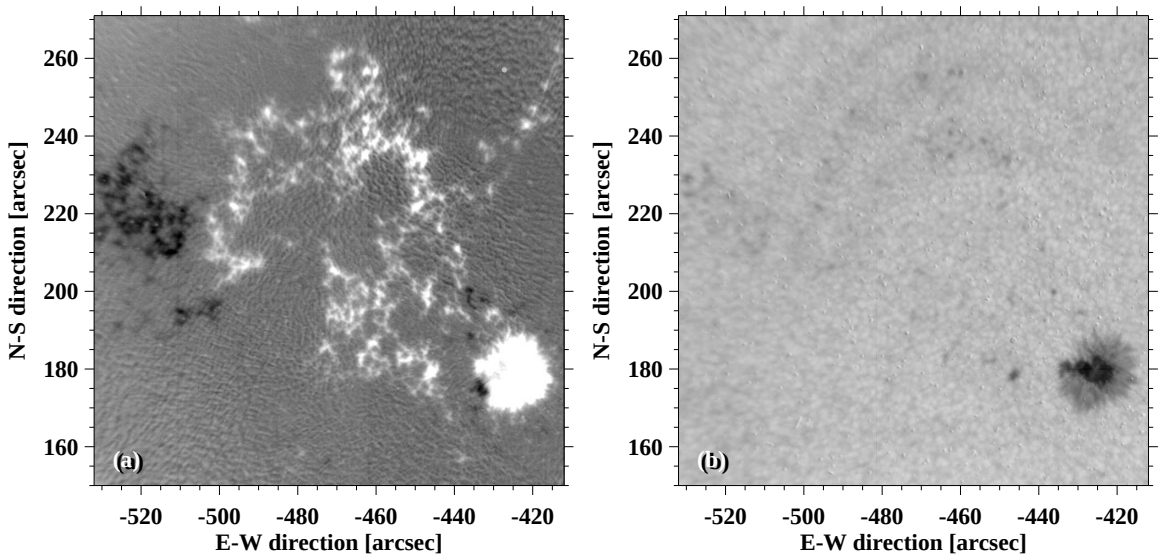

Fig. 2.— *Left*: Magnetogram of NOAA AR 10781 obtained with the BBSO IRIM at 16:00 UT on 2005 July 1. The FOV was $145'' \times 145''$. *Right*: Corresponding image of active region NOAA 10781 taken at the same time. The bandpass is 0.1 Å at 1.565 μm.

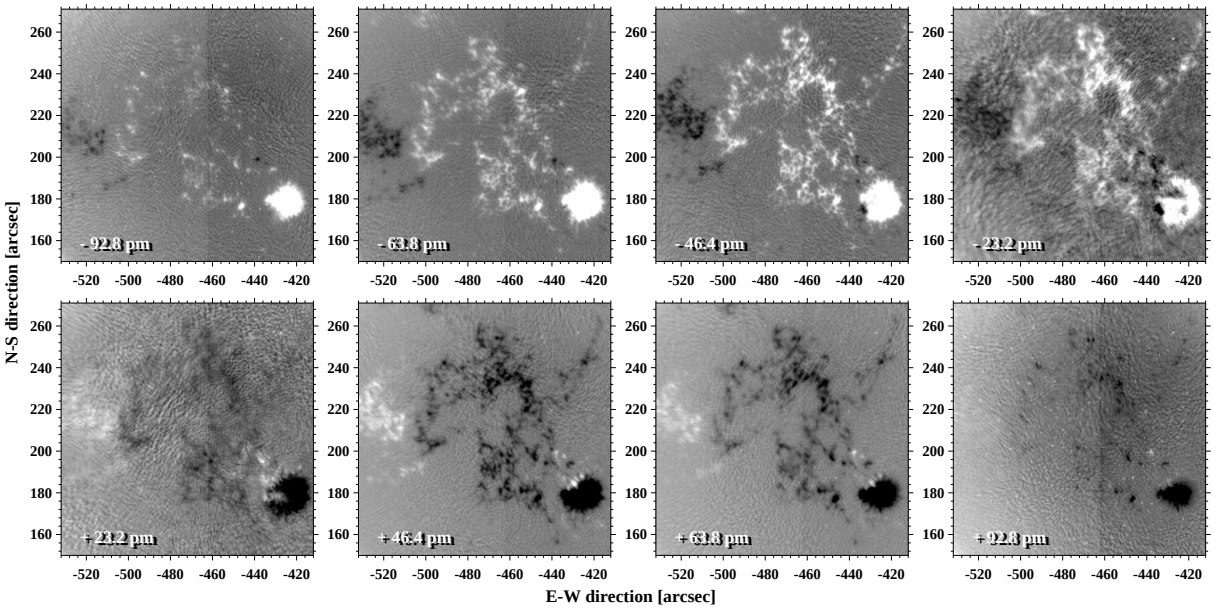

Fig. 3.— Spectral sequence of magnetograms of NOAA AR 10781 on 1 July 2005. Off-band wavelength values are marked at the bottom-left corner of each panel.

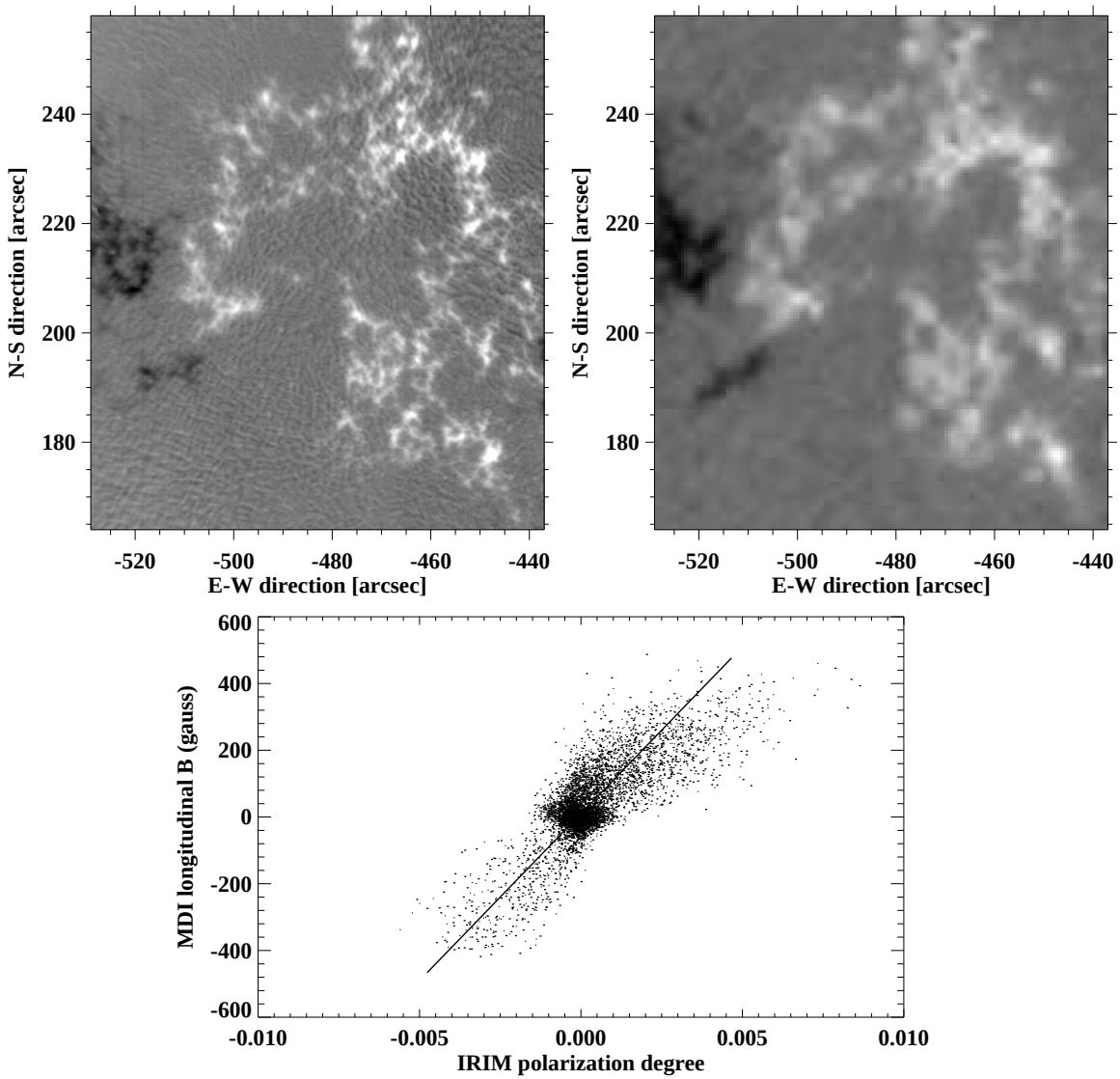

Fig. 4.— Magnetograms of NOAA AR 10781 obtained for comparison by (*left*) IRIM at 16:02 UT, (*right*) MDI at 16:00 UT. Scatter plot between IRIM and MDI magnetograms (*bottom*).

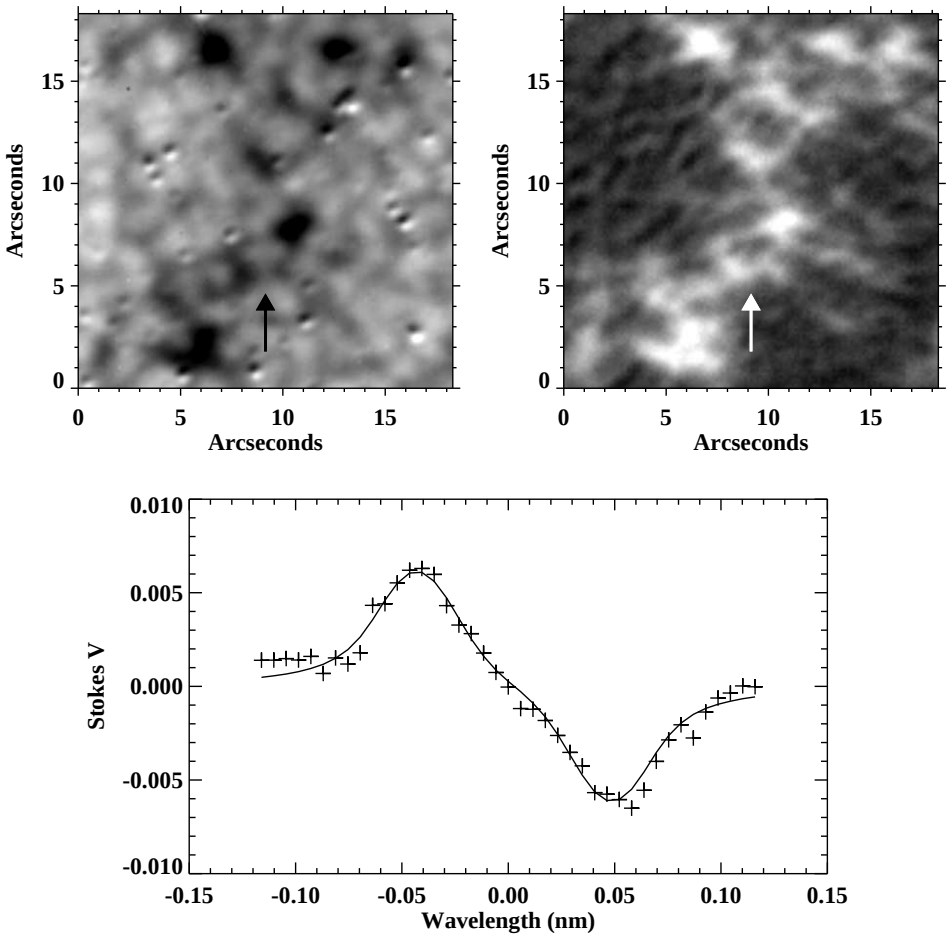

Fig. 5.— *Bottom*: Stokes V profile of a small-scale feature pointed by the arrow. *Right*: magnetogram taken at the same time. The FOV is $18'' \times 18''$. *Left*: Corresponding Stokes I image with 0.1 Å bandpass at 1.565 μm. The fitted intrinsic field strength is 482 gauss with a filling factor 49.3%, and the corresponding true magnetic flux is 2.04×10^{17} Mx.

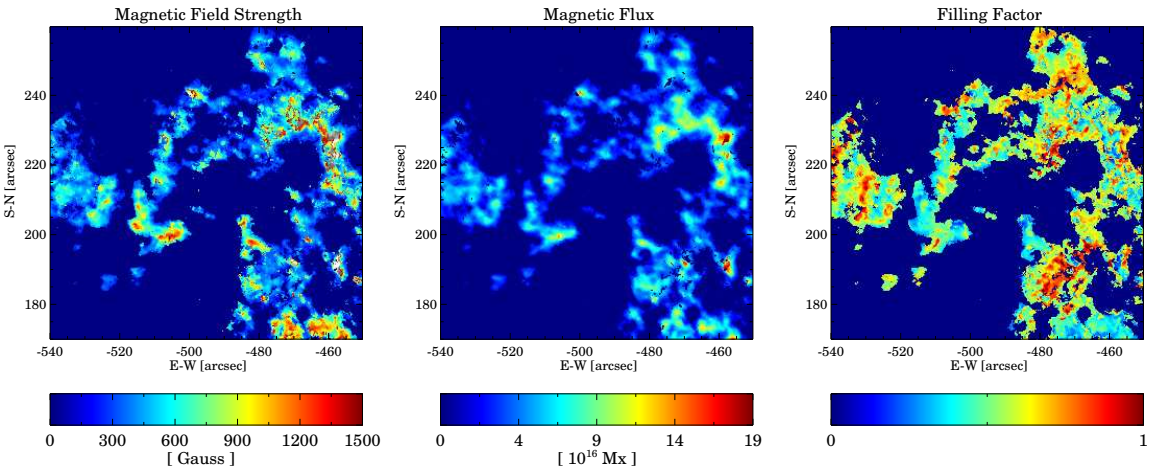

Fig. 6.— The true-field (*left*), magnetic flux (*middle*) and filling factor (*right*) maps of NOAA AR 10781. The corresponding color bars indicate the display ranges.

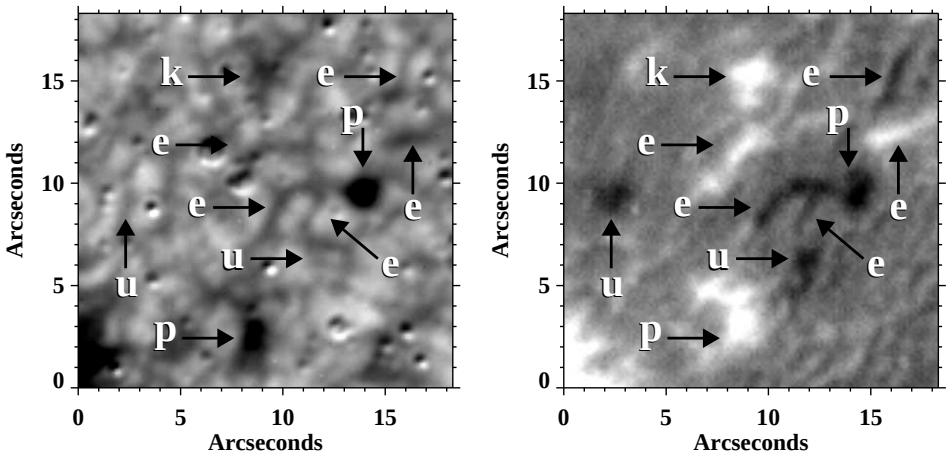

Fig. 7.— Detailed views of small-scale features illustrated in Figure 1. *Left*: Stokes I image with 0.1 Å bandpass at 1.565 μm. The dust on the surfaces of the Fabry-Pérot etalon fail to be cleaned by the dark and flat field corrections because of the telecentric configuration. *Right*: magnetogram taken at the same time. The FOV is $18'' \times 18''$. Small pores (marked by p), magnetic knots (marked by k), magnetic elements without correspondence (marked by u), as well as elongated magnetic structures (marked by e) are seen clearly, which demonstrates the polarimetry close to the diffraction limit of 65 cm telescope at 1.565 μm.

Table 1. Characteristic parameters of the IRIM Fabry-Pérot etalon at 1.565 μm

Etalon Properties		Etalon Parameters	
Diameter	70 mm	FSR	5.5 Å
Rough spacing	2226 μm	Bandpass	8.8 pm
Scanning range	4.1 μm	Finesse	62.8
Reflection	95.3%	Flatness	$\lambda/127$
Absorption	0.27%	Roughness	$\lambda/763$
Peak transmission	88.8%	Step scale	0.29 pm/step